Organophosphate hydrolase is a lipoprotein and interacts with pi-specific transport system to facilitate growth of brevundimonas diminuta using op insecticide as source of phosphate

Parthasarathy, Sunil; Parapatla, Hari; Nandavaram, Aparna; Palmer, Tracy; Siddavattam, Dayananda

Published in:
Journal of Biological Chemistry

DOI:
10.1074/jbc.M116.715110

Publication date:
2016

Document Version
Peer reviewed version

Organophosphate Hydrolase is a lipoprotein and interacts with P_i-specific transport system to facilitate growth of *Brevundimonas diminuta* using OP insecticide as source of phosphate.

Sunil Parthasarathy[1], Hari Parapatla[1], Aparna Nandavaram, Tracy Palmer[2] and Dayananda Siddavattam[1]

[1]Department of Animal Biology, School of Life Sciences, University of Hyderabad, Hyderabad- 500 046, Hyderabad, India.

[2] Division of Molecular Microbiology, College of Life Sciences, University of Dundee, Dundee, UK.

*****Running title: Organophosphate Hydrolase (OPH) is a lipoprotein

To whom correspondence should be addressed: Dayananda Siddavattam, Department of Animal Biology, School of Life Sciences, University of Hyderabad, Prof. C.R Rao Road, Gachibowli, Hyderabad, India 500 046, Tel.: +91 40 23134578; Fax: +91 40 23010120/145.
E-mail: sdsl@uohyd.ernet.in

Keywords: biodegradation, lipoprotein, protein complex, protein-protein interaction, multidrug transporter

---

ABSTRACT

Organophosphate hydrolase (OPH), encoded by the organophosphate degradation (*opd*) island, hydrolyses the triester bond found in a variety of organophosphate insecticides and nerve agents. OPH is targeted to the inner membrane of *Brevundimonas diminuta* in a pre-folded conformation by the Twin Arginine Transport (Tat) pathway. The OPH signal peptide contains an invariant cysteine residue at the junction of the signal peptidase cleavage site along with a well conserved lipobox motif. Treatment of cells producing native OPH with the signal peptidase II inhibitor globomycin resulted in accumulation of most of the preOPH in cytoplasm with negligible processed OPH detected in the membrane. Substitution of the conserved lipobox cysteine to serine resulted in release of OPH into the periplasm, confirming that OPH is a lipoprotein. Analysis of purified OPH revealed that it was modified with the fatty acids palmitate and stearate. Membrane-bound OPH was shown to interact with the outer membrane efflux protein TolC and with PstS, the periplasmic component of ABC transporter complex (PstSACB) involved in phosphate transport. Interaction of OPH with PstS appears to facilitate transport of P_i generated from organophosphates due to the combined action of OPH and periplasmically located phosphatases. Consisent with this model, *opd* null mutants of *B. diminuta* failed to grow using the organophosphate insecticide methyl parathion as sole source of phosphate.

This research was originally published in journal of biological chemistry. Sunil Parthasarathy, Hari Parapatla, Aparna Nandavaram, Tracy Palmer and Dayananda Siddavattam. Organophosphate Hydrolase Is a Lipoprotein and Interacts with Pi-specific Transport System to Facilitate Growth of Brevundimonas diminuta Using OP Insecticide as Source of Phosphate 2016; Vol:291 No. 14, pp. 7774-7785 © the American Society for Biochemistry and Molecular Biology."

Membrane-associated organophosphate hydrolase (OPH) hydrolyses the triester bond found in a variety of organophosphate insecticides and nerve agents (1,2). The 39 kDa monomer requires Zn^{+} ions as cofactor (3). OPH is encoded by the *opd* (organophosphate degrading) gene found on dissimilar plasmids and the *opd* gene has recently been shown to be a part of an Integrative Mobilizable Element (IME) (4). Due to the mobile nature of the *opd* island, identical *opd* genes are found among bacterial strains isolated from different geographical regions (4,5). Though its physiological substrate is unknown, OPH hydrolyzes paraoxon at a rate approaching the diffusion limit (kcat /KM 108 M^{-1} s^{-1}) (6). Considering its catalytic efficiency and broad substrate range, it has been assumed that OPH has evolved to degrade organophosphate (OP) insecticides accumulated in agricultural soils (7). Structural analysis shows that OPH contains a TIM barrel fold as seen in most of the members of amidohydrolase superfamily proteins (8).

OPH associates with cell membranes and membrane-associated OPH has been purified from a number of sources (3,9-13). Analysis of the amino acid sequences of OPH proteins indicates that all of them contain a predicted signal peptide harbouring a well-defined twin-arginine (Tat) motif. Twin-arginine signal peptides serve to target proteins to the twin-arginine protein transport (Tat) pathway which translocates folded proteins across the bacterial cytoplasmic membrane (14). ProteinaseK treatment confirmed that OPH is exported to the periplasmic side of inner membrane in *B. diminuta* and dependence on the Tat pathway was demonstrated since substitution of the invariant arginine residues of the Tat signal peptide affected both processing and localization of OPH (15). However, the mechanism by which OPH is anchored to the inner membrane and the physiological role of OPH are currently unclear. In this report we demonstrate that OPH is a lipoprotein and that it plays an essential role in the acquisition of phosphate from OP insecticides.

EXPERIMENTAL PROCEDURE

Media, Strains and plasmids- Strains and plasmids used in the present work are shown in Table 1. Primers used for PCR amplification and site-directed mutagenesis are listed in supplementary Table 1. *B. diminuta* cultures were grown either in LB medium or in HEPES minimal medium. HEPES minimal medium was prepared by dissolving 0.2 g KCl, 0.2 g $MgSO_4.7H_20$, 40 mg $CaNO_3.4H_2O$, 80 mg $(NH_4)_2HPO_4$ and 1 mg Fe_2SO_4 in a litre of 50 mM HEPES, pH 7.4. The medium also contained essential amino acid mixture (0.07 mM), pantothenate (0.5 mg), vitamin B-12 (0.001 mg) and biotin (0.001 mg) along with sodium acetate (2%) as carbon source. The $(NH_4)_2HPO_4$ was omitted when methyl parathion (0.6 mM) was used as sole phosphate source. When required polymyxin (10 µg/ml), chloromphenicol (30 µg/ml) or tetracycline (20 µg/ml) were supplemented to the growth medium. All chemicals used in this study were procured from Sigma-Aldrich, Bengaluru, unless otherwise specified all restriction and other enzymes used in DNA manipulations were procured from ThermoScientific, USA. Routine DNA manipulations were performed following standard procedures (16).

Carbonate and urea extraction- Total membrane preparations were made from *B. diminuta* by following standard procedures (17). The cytoplasmic membrane was isolated by following the discontinuous sucrose gradient method described elsewhere (18) and equal amounts of membrane was resuspended in buffer containing different concentrations of sodium carbonate, pH 11.5, or urea (2-8 M as indicated). After 1 h incubation at room temperature the samples were centrifuged at 227,226 x *g* using a TLA 120.2 rotor (Beckman coulter) for 45 min to pellet the washed membranes. Detection of OPH in the wash supernatant and membrane fractions

was achieved by western blots using anti-OPH antibodies (15). The quantity of OPH in membrane and supernantant fractions were densitometrically determined by comparing with the OPH signal obtained with untreated membrane.

Globomycin treatment- The *opd* null mutant, *B. dimimuta* DS010 containing the plasmid pSM5 was grown in LB medium to mid log phase (0.6 OD at 600 nm) and 50 µg/ml globomycin (Sigma-Aldrich) was added to the culture medium 1 h before the expression of OPH was induced by addition of 3 mM isopropyl β-D-galactopyranoside (IPTG) (19,20). After 6 h of induction, the culture was harvested, washed in SET buffer (500 mM Sucrose, 5 mM EDTA and 20 mM Tris-HCl, pH 8.0) and used to prepare periplasmic, cytosolic and total membrane fractions as described previously (21,22). OPH specific signals in the subcellular fractions were detected by performing western blot analysis.

Generation of OPH^{C24S}- The invariant cysteine residue in the lipobox motif of the OPH signal peptide was modified to serine by performing quikchange™ site directed mutagenesis (Stratagene). Plasmid pMS5 was used as template and the cysteine to serine codon substitution was confirmed by sequencing. The resulting plasmid coding for OPH^{C24S} was designated pCSOPH. The *B. diminuta* DS010 (pCSOPH) cultures were grown to mid log phase and the expression of OPH^{C24S} was induced overnight by supplementation with 3 mM IPTG. The cells expressing OPH^{C24S} were subsequently harvested, washed and fractionated into periplasm, cytoplasm and total membrane for the detection of OPH. A similar fractionation procedure was undertaken with *B. diminuta* DS010 (pSM5) to assess membrane anchorage of OPH in wild type cells.

Solubilization of OPH from the inner membrane- Inner membrane preparations were isolated from a 10 l overnight culture of *B. diminuta* following procedures described elsewhere (18). The isolated inner membrane was resuspended in minimal amounts of buffer (20 mM Tris-HCl, pH 8.0, 150 mM NaCl, 2% glycerol) and after estimating protein concentration the buffer volume was adjusted to give a final protein concentration of 5 mg/ml. Triton X-100 (2g/g protein), Triton X-114 (2g/g protein), n-Dodecyl β-D-maltoside (DDM) (1g/g protein) and digitonin (8g/g protein) were separately added to aliquots of the membrane suspension and samples were incubated with gentle rotation (10 rpm) for 1 h at 4ºC. Subsequently, the samples were subjected to ultracentrifugation (117,000 x *g*) and the clarified supernatants, containing solubilised protein, were removed into prechilled tubes. The detergent insoluble fraction was resuspended in an equal volume of buffer and the OPH activity was estimated in both detergent soluble and detergent insoluble fractions (3). The percent OPH release from the membrane was calculated by comparing with total OPH activity associated with the untreated membrane. Subsequently, for identification of fatty acids attached to OPH, the protein was solubilized using 1.5% Triton X-100 as it disrupts interactions of OPH with other proteins and facilitates purification of OPH without interacting partners.

Affinity purification of OPH and identification of fatty acids- For purification of OPH-specific antibodies, 10 mg of pure OPH, purified as described elsewhere (23), was coupled to 400 µl of CNBr-activated Sepharose™ 4B (GE healthcare) following the manufacturer's protocol. Aliquots of OPH antisera (15) were passed through the OPH-coupled Sepharose column at a flow rate of 0.5 ml per minute. The flow-through was collected carefully and reloaded onto the column to ensure complete binding of OPH-specific antibodies to the column. The unbound antibodies and serum proteins were removed by washing the column with three column volumes of wash buffer (20 mM Tris-HCl, pH 7.6). The bound anti-OPH antibodies were eluted (0.1 M glycine-HCl, pH 2.5) as 1 ml fractions into pre-chilled tubes containing 100 µl of 1 M Tris-HCl,

pH 9.0 to ensure quick neutralization of the eluate. The antibody fractions were then pooled and dialyzed against coupling buffer (10 mM sodium phosphate, pH 7.2, 150 mM NaCl).

For coupling to proteinA/G beads, Approximately 1 mg of purified anti-OPH antibodies were mixed with 500 µl protein A/G-agarose plus beads (ThermoScientific) equilibrated with coupling buffer and kept for 1 hour at 4^0C with gentle shaking. The contents were loaded on to a column and the excess unbound antibodies were removed by washing the column with three column volumes of coupling buffer. The anti-OPH antibodies bound to protein A/G-agarose beads were covalently linked by adding one column void volume of cross-linking buffer (10 mM Sodium phosphate, pH 7.2, 150 mM NaCl), 2.5 mM disuccinimidyl suberate (DSS) to the column. The column was left for one hour at room temperature to complete cross-reaction and the excess DSS were quenched by washing the column with 25 mM Tris-HCl, pH 7.6. The OPH-antibody cross-linked protein-A/G agarose beads were then taken into a clean tube and suspended in 1 ml of prechilled binding buffer (20 mM Tris-HCl, pH 7.6, 150 mM NaCl, 2% glycerol). Immediately, Triton X-100 solubilised membrane proteins of *B. diminuta* were added to the beads and left overnight at 4^0C with head to head rotation. After incubation the contents were loaded onto a column, washed thoroughly with wash buffer and the bound proteins were then eluted with glycine-HCl, pH 2.5 prior to neutralization with 100 mM Tris-HCl, pH 9.0. About 100 µg of immuno-purified OPH was esterified using methanolic-HCl (24). The fatty acid methyl esters generated from OPH were then analyzed using Agilent GC/MS equipped with a quadrupole mass selective detector. Control samples were prepared from the periplasmic fraction of *B. diminuta* DS010 (pCSOPH) and treated identically to identify the fatty acid methyl esters.

Identification of the OPH interactome- To identify interacting proteins, OPH was affinity purified using two different approaches. Before proceeding with the purification of OPH, the cell pellet collected from wild type *B. diminuta* was resuspended in PBS buffer (1g/10ml) before treatment with 25 mM formaldehyde (25,26). The formaldehyde cross-linked cell pellet was sonicated (10 cycles of 20 sec ON and 40 sec OFF) and the membrane fraction was isolated following established procedures (27). The membrane pellet was extracted three times with 5 ml chloroform:methanol (3:1) and the precipitated proteins were resolubilized in phosphate buffer (0.1 M Phosphate buffer, pH 7.6, 350 mM NaCl, 5% glycerol, 1% DDM and 50 mM Imidazole). The first approach involved immunopurification using anti-OPH antibody cross-linked protein-A agarose beads. The resolubilized cross-linked OPH complex was passed through the column containing the antibody-linked beads at a flow rate of 0.5 ml/minute. The flow through was repeatedly passed through the column until negligible amounts of protein were detected flowthrough sample. After washing the column with three column volumes of wash buffer (20 mM Tris-HCl, pH 7.6, 150 mM NaCl, 2% glycerol, 0.1% DDM), the bound cross-linked OPH complex was eluted as described above, and subsequently analyzed both under native and denaturing conditions. Blue native PAGE (28) and gel filtration (Superose 6, 10/300 GL, GE healthcare) were performed to assess the molecular mass of the OPH complex and Tricine-PAGE (29) was performed to visualise polypeptides coeluting with OPH.

In an alternative approach, a deca-histidine tagged OPH variant (OPH^{10xHis}) was generated. To achieve this, a DNA fragment encoding 10 histidine residues was introduced into the *opd* gene, between nucleotide positions 420 and 426 that encodes amino acids in a loop region of OPH. First, a *Bam*HI restriction site was introduced into *opd* by performing quick change mutagenesis between nucleotide positions 420-426 using plasmid pSM5 as template. Next, the synthetic DNA fragment encoding the ten histidine

residues was prepared as a *Bgl*II fragment and inserted in-frame into the *opd* gene at the generated *Bam*HI site. The resultant plasmid was designated pOPH141HIS. Plasmid pOPH141HIS was mobilized into *B. diminuta* DS010, and *B. diminuta* DS010 (pOPH141HIS) cells were then induced to express OPH^{10xHis} by addition of IPTG at a final concentration of 3 mM. After incubation with IPTG for 5 h the cells were harvested and the cell pellet was resuspended in PBS buffer (1g/10ml) and treated with 25 mM formaldehyde to cross-link OPH. The formaldehyde cross-linked cell pellet was processed as described earlier to obtain total membrane pellet. The pellet was then extracted three times with 5 ml chloroform:methanol (3:1) and the precipitated proteins were resolubilized before loading the soluble proteins onto a Ni-charged immobilised metal affinity column (IMAC). Following washing with phosphate buffer, bound protein was eluted with 500 mM Imidazole in phosphate buffer and analyzed both on blue native and Tricine-PAGE. The affinity purified OPH complexes were subjected to tryptic digestion and mass spectrometry (LTQ-Orbitrap XL ETD mass spectrometer) as described elsewhere (30) to establish the identity of OPH interacting proteins.

Bacterial two Hybrid system- Protein-protein interactions were studied by the bacterial two-hybrid system (BACTH, Euromedex) following protocols described elsewhere (31). The T25 and T18 domains were separately fused to the N or C termini of the target proteins (OPH and PstS). The fusions were produced independently by cloning the *opd* and *pstS* genes in either pKNT25 or pUT18C. Cells of *Escherichia coli* strain BTH101 (Euromedex) were transformed with different combinations of fusion plasmids i.e. pUT18CPstS-pKNT25OPH and pUT18COPH-pKNT25PstS. The combinations pUT18CPstS-pKNT25 and pUT18COPH-pKNT25 served as controls. β-galactosidase assay was performed as described elsewhere (32).

Pull-down assay of coexpressed proteins: Interaction of OPH with phosphate binding protein, PstS and efflux pump component, TolC, was determined by performing coexpression-pull-down assays (33). Initially, an *opd* gene variant engineered to code for OPH with C-terminal AviTag was generated. Two complementary oligos specifying the AviTag sequence (AviTag-F and AviTag-R; Supplementary Table 1) were annealed, digested with *Xho*I and *Hind*III and cloned into similarly-digested plasmid pSM5 to give plasmid pOPHV400 – this procedure results in insertion of the AviTag coding sequence in frame with *opd*. Next, the *opd* gene from plasmid pOPHV400 was excised as an *Eco*RI and *Hind*III fragment and cloned into one of the multiple cloning sites of pETduet1 vector that had been similarly digested. Subsequently, the *birA* gene was cloned as an *Nde*I and *Xho*I fragment into the second multiple cloning site of this construct. The cloning strategy places *birA* under the control of T7 promoter, allowing for regulatable expression of biotin ligase, the enzyme required to ligate biotin at the conserved lysine residue of the AviTag. The resulting pETduet1 derivative, designated pAVB400, codes for both $OPH^{CAviTag}$ and the biotin ligase. The *pstS* gene was amplified from *B. diminuta* and cloned initially in pET23b as an *Nde*I-*Xho*I fragment. The generated recombinant plasmid, pPST300, codes $PstS^{C6His}$. After confirming expression of $PstS^{C6His}$, *pstS* was amplified from pPST300 using primers PstSPMB-F and PstSPMB-R, respectively, and cloned into similarly digested pMMB206 to give plasmid pLPST300, which encodes $PstS^{C6His}$ controlled by the *tac* promoter of the vector. *E. coli* ArcticExpress cells harbouring pAVB400 were transformed with pLPST300 and the expression of $OPH^{CAviTag}$ and $PstS^{C6His}$ was induced following standard procedures. The total cell lysate was prepared and the clear lysate was used to isolate $OPH^{CAviTag}$ and any interacting partners using streptavidin magnetic beads (Dynabeads M-280 Streptavidin, Invitrogen) following the

manufacturer's protocols. The proteins bound to magnetic beads were analyzed by 12.5% SDS-PAGE and probed either with anti-OPH or anti-His antibodies to detect $OPH^{CaviTag}$ and $PstS^{C6His}$. Cell lysates prepared either from ArcticExpress (pAVB400) or ArcticExpress (pLPST300) cells treated in similar manner served as controls.

OPH-TolC interactions: The *tolC* gene was amplified from *B. diminuta* and cloned as a *Bgl*II-*Eco*RI fragment into similarly digested pRSETA. As the cloning strategy facilitates in frame fusion of the vector-specified His-tag to *tolC*, the resulting recombinant plasmid, pTOLC400 codes for $TolC^{N6His}$. Similarly, the *opd* gene was amplified from *B. diminuta* as an *Eco*RI-*Hind*III fragment and cloned into similarly digested pMMB206. The resulting recombinant plasmid, pTLOPH, codes for OPH without any affinity tag, expressed under control of the *tac* promoter. The $TolC^{N6His}$ and OPH were coexpressed by adding 1 mM of IPTG to the mid log phase cultures of ArcticExpress (pTLOPH400 + pTOLC400). Similarly, the expression of $TolC^{N6His}$ and OPH were induced from ArcticExpress (pTLOPH400) and ArcticExpress (pTLOPH400) cells before preparing clear lysate (4 ml) from 50 ml of culture. The lysate was then incubated overnight with 20 µl of MagneHis beads (Promega) at 4^0C with constant mixing. After incubation, the beads were collected and washed following the manufacturer's protocol and the presence of $TolC^{N6His}$ and OPH were detected by performing immunoblots probed either with anti-OPH antibodies or anti-His antibodies.

RESULTS

OPH is tightly bound to the B. diminuta inner membrane- It has previously been demonstrated that OPH is associated with the inner membrane of *B. diminuta* (15). To probe the nature of the interaction of OPH with the membrane, we first determined whether the protein could be released from membrane fractions following washing under alkaline conditions using sodium carbonate (Fig. 1*A*), or under strong denaturing conditions in the presence of urea (Fig. 1*B*). At concentrations of sodium carbonate normally used to extract peripheral membrane proteins (0.1-0.5M) (34), very little OPH was released from the membrane, suggesting a relatively tight association with the bilayer. However at higher concentrations of carbonate, significant levels of OPH were released (Fig. 1*A*). Likewise the protein was also relatively refractory to extraction by urea, with most of the protein remaining associated with the membrane fraction even in the presence of 8 M urea (Fig. 1*B*). This behaviour is consistent with OPH being an integral protein of the inner membrane rather than associating with the membrane by electrostatic interaction or through binding to other inner membrane proteins.

OPH is a lipoprotein- The Tat system is known to assemble some membrane-anchored proteins (20,35,36). In bacteria these usually have either a single transmembrane domain at the C-terminus (35) or an N-terminal non-cleaved twin-arginine signal anchor sequence (37). However, bioinformatic analysis supported by structural studies show that OPH has no C-terminal hydrophobic helical domain (38) and the N-terminal signal peptide of OPH is cleaved off during biosynthesis and therefore cannot serve as a signal anchor (15).

A third class of bacterial membrane proteins that is known to be assembled by the Tat pathway is lipoproteins (20,39,40). *In silico* analysis of the OPH signal peptide, shown in Fig. 2*A*, predicts the existence of both a SpaseII and multiple SpaseI cleavage sites in pre-OPH, with the SpaseII cleavage site predicted with the highest level of confidence. In addition to the predicted SpaseII cleavage site, a well conserved lipobox containing a cysteine residue was found in the c-region of the signal peptide (Fig. 2*A*). To determine whether OPH was a substrate of Spase II, we treated cells of *B diminuta* DS010 (pSM5) with globomycin, which inhibits processing of the

prolipoprotein by binding irreversibly to the peptidase (20,41). In support of the *in silico* prediction, in the globomycin-treated cultures most of the OPH accumulated in the cytoplasmic fraction in an unprocessed form (Fig. 2*B*, lane 1). This is in contrast with the untreated cells where very little precursor was detectable (Fig. 2*B*, lane 2). Moreover, there was substantially less mature OPH detectable in the membrane fraction following globomycin treatment (Fig 2*B*, lane 3).

To provide additional evidence that OPH is a lipoprotein, we generated a serine substiution of the essential cysteine in the OPH signal sequence lipobox (OPH^{C24S}) and compared the subcellular location of this variant to that of the wild type protein (Fig. 2*C,D*). Unlike the wild type protein where the mature form is found in membrane fraction (Fig. 2*C*), most of the processed form of OPH^{C24S} was found in periplasm, with very little seen in the membrane (Fig. 2*D*). Since SpaseII acts only on acylated prolipoproteins to generate S-lipidated cysteine at the N-terminus of the mature protein (42), it is assumed that the mature-sized form of OPH^{C24S} found in periplasmic fraction results from processing by SpaseI (Fig. 2*A*), which is predicted bioinformatically to recognise this signal peptide (Fig. 2*A*). Taken together these results demonstrate that OPH is a membrane-anchored lipoprotein.

Mature OPH is linked to myristic and oleic fatty acids- Previous findings have shown that generally diacyl glycerol serves as a lipid anchor for membrane-associated lipoproteins (43). To confirm the nature of the lipid anchor on membrane-bound OPH and to identify the fatty acid modifications, we extracted fatty acids from affinity purified OPH and OPH^{C24S} (as a negative control) using methanolic-HCl extraction (24). The fatty acid methyl esters generated due to transesterification were extracted and analyzed using GC-MS. As shown in Fig. 3*A* and *B*, two novel peaks were identified arising from the mOPH purified from *B. diminuta* membranes, which were not observed in the control sample derived from OPH^{C24S}. These two peaks corresponded to methyl myristate (C14: 0) and methyl oleic acid (C18: 1) with 97% and 99% identities (Fig. 3, *C, D, E* and *F*). These results demonstrate that OPH is anchored to the membrane through diacyl-glycerol which is linked with myristic and oleic groups.

OPH interacts with phosphate ABC transporter- To gain further clues about the physiological role of OPH, we next sought to identify whether it interacted with other cellular proteins. First we developed a strategy to purify OPH in its native state by dispersing the membrane fraction with the non-ionic detergents Triton X-114, n-Dodecyl β-D-maltoside (DDM) and digitonin. Of the three detergents, DDM facilitated the best release of OPH (liberating approximately 70% of total OPH; data not shown).

Next, we developed a strategy to purify DDM-solubilised OPH. In the crystal structure of OPH the C-terminal region is exposed (38), and we therefore constructed a strain of *B. diminuta* producing OPH with a C-terminal Hexa histidine tag. However the DDM-solubilised OPH^{C6His} failed to bind the Ni-NTA column, suggesting that the C-terminus of OPH is not able to interact with the affinity matrix, possibly due to masking of this region by a partner protein subunit. To resolve this problem, we again used the crystal structure of OPH as a reference to introduce an internal decahistidine tag internally into a loop region of OPH. This variant, designated OPH^{10xHis}, bound well to the Ni-affinity matrix following solubilisation from the membrane. The affinity-purified OPH^{10xHis} sample was further analyzed both by BN-PAGE and gel filtration. These two independent experiments both suggested that OPH^{10xHis} was present in a complex of around 294 kDa (Fig. 4*A* and *B*). Assuming that the detergent used to solubilise OPH from the membrane may interfere with the determination of an accurate molecular mass for the OPH complex, the isolated membranes from the formaldehyde treated *B. diminuta* DS010 (pOPH141HIS) cells were

extracted with methanol:chloroform (3:1) to delipidate the sample and the resulting membrane protein precipitate was resolubilised before proceeding with affinity purification of the cross-linked OPH-complex. BN-PAGE analysis of the OPH-complex isolated in this way coincided with the mass of the OPH complex purified from detergent-solubilized membranes (compare Fig. 4*B* with Fig. 4*C*, lane 1).

To validate these findings were employed a second, independent approach to purify untagged OPH. The membranes isolated from the formaldehyde cross-linked *B. diminuta* wild type cells were extracted with methanol:chloroform (3:1) and the resolubilised membrane proteins were passed through a protein-A column that had been crosslinked with OPH-specific antibodies. The size of the OPH complex obtained following this purification process coincided with the BN-PAGE profile of the OPH complex purified following Ni-affinity column (IMAC) (Fig. 4*C*, lane 3). We therefore conclude that OPH is present in an approximately 293 kDa complex.

The delipidated OPH complexes purified by immuno-affinity and by IMAC were analysed by Tricine-SDS-PAGE. It can be seen (Fig. 4*D*) that several protein bands with similar sizes are common between the two samples, although bands with apparent masses of 38 kDa, 35 kDa and 15 kDa are more intense in immuno-purified OPH complex. The 35 kDa protein coincided with the size of OPH and its identity was also established by performing a western immunoblot with anti-OPH antibodies (Fig. 4*D*).

After establishing that OPH is a multiprotein complex, we performed mass-spectrometry to obtain unique peptide sequences from proteins copurifying with OPH following IMAC. The obtained peptide sequences were identified using either x!tandem or Mascot web servers. Proteins that matched with more than two peptide sequences are listed in Table 2. From the list of proteins, subunits of the F_1F_oATP synthase (α, β, γ), the phosphate ABC transporter substrate binding protein (PstS) and efflux pump components AcrB and TolC were identified as candidate OPH interacting partners (Table 2). It is interesting to note that the identified peptides matched with proteins involved either in phosphate uptake (44) or in effluxing of xenobiotics (45), as organophosphates are xenobiotics that also contain a potential source of phosphate.

OPH interacts with phosphate specific transport component PstS- As PstS is a periplasmic protein that binds specifically to inorganic phosphate, we chose to further probe potential interaction of OPH with PstS. Initially we undertook bacterial two-hybrid analysis to assess OPH-PstS interactions. When PstS was fused to the C-terminus of the adenylate cyclase T18 fragment and OPH to the N-terminus of the T25 fragment, adenylate cyclase activity was reconstituted, and strong β-galactosidase activity could be measured (Fig. 5*A*). A similar strong interaction was also seen when OPH was fused to the C-terminus of the adenylate cyclase T18 fragment and PstS to the N-terminus of the T25 fragment. To confirm that OPH and PstS directly interact, we performed coexpression-pulldown assays. To this end we generated compatible plasmids coding for $OPH^{CAviTag}$ (pAVB400) and $PstS^{N6His}$ (pPST300). In addition, plasmid pAVB400 also codes for the biotin ligase, BirA, to facilitate ligation of biotin at the conserved lysine residue of AviTag found at the C-terminus of $OPH^{CAviTag}$. After inducing the production of $OPH^{CAviTag}$, $PstS^{N6His}$ and biotin ligase in the heterologous host *E. coli*, Streptavidin-linked beads were used to isolate biotinylated $OPH^{CAviTag}$. As shown in Fig. 5*B*, $PstS^{N6His}$ copurified with the biotinylated $OPH^{CAviTag}$ (Fig. 5*B*, lane 1), but was not purified by the Streptavidin-linked beads in the absence of $OPH^{CAviTag}$ (Fig. *5B*, lane 3), providing conclusive proof that OPH and PstS are interaction partners.

Efflux pump component TolC interacts with OPH: Analysis of the OPH interactome

indicated that efflux pump components AcrA, AcrB and TolC also copurified with OPH isolated from *B. diminuta* (Table 2). We next sought to assess whether there was a direct interaction between OPH and any of these three proteins by heterologous expression and pairwise copurification studies. Unfortunately, we were unable to express *B. diminuta* AcrA and AcrB in *E. coli*. However, TolC with an N-terminal His-Tag was successfully produced in the *E. coli* ArcticExpress strain. We therefore coexpressed untagged OPH along with $TolC^{N6His}$ and isolated $TolC^{N6His}$ from total cell lysates using MagneHis beads. Fig. 5*C* shows that when $TolC^{N6His}$ was affinity purified, the mature form of OPH was also copurified (Fig.5*C*, lane 1). Since OPH produced in the absence of $TolC^{N6His}$ was unable to interact with the beads (Fig.5*C*, lane 2), it can be concluded that OPH and TolC can directly interact with each other.

OPH supports B. diminuta growth with methyl parathion as sole phosphate source: The enzymatic action of OPH generates alkyl phosphates from a variety of organophosphate insecticides due to its triesterase activity (3). These diesters, like diethyl phosphate, may serve as substrates for periplasmically located phosphatases/diesterases, ultimately generating inorganic phosphate (P_i), raising the possibility that interaction of OPH with PstS facilitates the transport of generated inorganic phosphate into the cell. To examine this further, we investigated the ability of *B. diminuta* to grow in minimal medium using the OP insecticide methyl parathion as sole source of phosphate. As shown in Fig. 6, *B. diminuta* DS010 alone was unable to grow using methyl parathion as phosphate source, but when carrying plasmid pSM5, encoding OPH, good growth was seen. These results show that OPH is required to support growth using organophosphates as a source of phosphate.

DISCUSSION

In this study we have investigated the interaction of the organophosphate hydrolase, OPH, from *B. diminuta*, with the cytoplasmic membrane and with other cellular proteins. Our work has clearly shown that OPH is a lipoprotein, and adds to a growing list of Tat-dependent lipoproteins in bacteria and archaea (20,44,47). Interestingly, OPH contains an alanine residue at the +2 position and according to the sorting rules for *E. coli* lipoproteins (42) should be translocated to the outer membrane by the Lol machinery (the genes for which are found in the genome of *B. diminuta*). However, a number of exceptions to these sorting 'rules' have been seen in other Gram negative bacteria, for example in *Pseudomonas aeruginosa* where lipoproteins having lysine, glycine and glutamine at + 2 position remain attached to the inner membrane (49). It appears for *B. diminuta* an alanine at +2 position also permits inner membrane retention.

Copurification studies using two independent approaches showed that OPH was present as a large multi-protein complex that includes other inner membrane proteins such as a predicted PhoR-like histidine kinase, periplasmic proteins such as PstS and outer membrane proteins TolC and AcrA. Further support for an OPH complex was provided by demonstrating a direct interaction between OPH and PstS, and between OPH and TolC. Growth studies showed that the indirect liberation of organic phosphates from methyl parathion mediated by OPH can support growth with this compound as sole phosphate source. These findings point to a potential model whereby the triesterase activity of OPH generates phosphodiesters from a variety of OP insecticides which are converted to inorganic phosphates by periplasmically-located phosphatases (Fig. 7). The PstS protein, identified here as an interacting partner of OPH, is a known component of an established phosphotransfer system (44), and it binds to inorganic phosphate, facilitating its transport across the inner membrane. During OPH-mediated hydrolysis of OP insecticides, in

addition to alkyl phosphates, aromatic compounds like *p*-nitrophenol are also generated. Products such as *p*-nitrophenol are more toxic than the parent compounds and if they are not quickly metabolized they need to be effluxed for the survival of the organism. In this context, OPH interactions with efflux pumps may serve to quickly eliminate toxic degradation products from the intracellular environment.

Acknowledgements: SP acknowledges Shantha Biotechnics for providing Junior Research Fellowship (JRF) and British Council, UK for the award of Commonwealth Split-Site Fellowship. Research support given by DBT to DS laboratory is highly acknowledged. Animal Biology is a DST-FIST supported Department. The School of Life Sciences, University of Hyderabad is supported by DBT-CREBB/BUILDER.

Conflict of interest: The authors declare that they have no conflicts of interest with the contents of this article.

Author contributions: SP, HP and AN performed the experiments. TP and DS conceived the idea and drafted the manuscript.

REFERENCES

1. Cho, C. M., Mulchandani, A., and Chen, W. (2002) Bacterial cell surface display of organophosphorus hydrolase for selective screening of improved hydrolysis of organophosphate nerve agents. *Appl. Environ. Microbiol*. **68**, 2026–2030
2. Efrmenko, E. N., and Sergeeva, V. S. (2001) Organophosphate hydrolase- an enzyme catalyzing degradation of phosphorus-containing toxins and pesticides. *Russ. Chem. Bull* (Int Ed). **50**, 1826–1832
3. Dumas, D. P, Caldwell, S. R., James R. Wild, and Frank M. Raushel (1989) Purification and Properties of the Phosphotriesterase from *Pseudomonas diminuta*. *J. Biol. Chem.* **264**, 19659-19665
4. Pandeeti, E. V. P., Longkumer, T., Chakka, D., Muthyala, V. R., Parthasarathy, S., Madugundu, A. K., Ghanta, S., Medipally, S. R., Pantula, S. C., Yekkala, H., and Siddavattam, D. (2012) Multiple Mechanisms Contribute to Lateral Transfer of an Organophosphate Degradation (*opd*) Island in *Sphingobium fuliginis* ATCC 27551. *G3 (Bethesda)* **2**, 1541-1554
5. Pandeeti, E. V. P., Chakka, D., Pandey, J. P., and Siddavattam, D. (2011) Indigenous organophosphate-degrading (opd) plasmid pCMS1 of *Brevundimonas diminuta* is self-transmissible and plays a key role in horizontal mobility of the *opd* gene. *Plasmid* **65**, 226-231
6. Omburo, G. A., Kuo J. M., Mullins L. S and Raushel F. M. (1992) Characterization of the zinc binding site of bacterial phosphotriesterase. *J. Biol. Chem*. **267**, 13278-13283
7. Walker, C. H. (1993) The classification of esterases which hydrolyse organophosphates: Recent developments, *Chem-Biol. Interact*. **87**, 17-24
8. Bigley, A. N and Raushel, F. M. (2013) Catalytic Mechanisms for Phosphotriesterases, *Biochim. Biophys. Acta.* **1834**, 443–453
9. Brown, K. A. (1980) Phosphotriesterases of *Flavobacterium* sp. *Soil. Bio. Biochem*. **12**, 105-12
10. Chaudhry, G. R., Ali, A., and Wheeler. W. B. (1988) Isolation of a methyl parathion-degrading *Pseudomonas* sp. that possesses DNA homologous to the *opd* gene from a *Flavobacterium* sp. *Appl. Environ. Microbiol*. **54**, 288-293
11. Serdar, C. M., Gibson, D. T., Munnecke, D. M. And Lancaster, J. H. (1982) Plasmid involvement in parathion hydrolysis by *Pseudomonas diminuta*. *Appl. Environ. Microbiol*. **44**, 246–249
12. Mulbry, W. W., and Karns, J. S. (1989) Purification and characterization of three parathion hydrolases from Gram-negative bacterial strains. *Appl. Environ. Microbiol*. **55**, 289-295

13. Siddavattam, D., Khajamohiddin, S., Manavathi, B., Pakala, S. B., and Merrick. M. (2003) Transposon-like organization of the plasmid-borne organophosphate degradation (*opd*) gene cluster found in *Flavobacterium* sp. *Appl. Environ. Microbiol*. **69**, 2533-2539
14. Palmer, T., and Berks, B. C. (2012) The twin-arginine translocation (Tat) protein export pathway. *Nat. Rev. Microbiol*. **10**, 483-496
15. Gorla, P., Pandey, J. P., Parthasarathy, S., Merrick, M. and Siddavattam, D. (2009) Organophosphate hydrolase in *Brevundimonas diminuta* is targeted to the periplasmic face of the inner membrane by the twin arginine translocation pathway. *J. Bacteriol.* **191**, 6292–6299
16. Sambrook, J. Russell DW (Ed), Molecular Cloning: A Laboratory Manual (2001), 1st ed. Cold Spring Harbor Laboratory Press, Cold Spring Harbor. Cold Spring Harbor Laboratory, Cold Spring Harbour, NY
17. Kaback, H.R. (1971) Bacterial membranes. *Methods. Enzymol*. **22**, 99–120
18. Schnaitmann, C. A. (1970). Protein composition of the cell wall and cytoplasmic membrane of *Escherichia coli*. *J. Bacteriol*. **104**, 890-901
19. Zwiebel, J. L., Inukai, M., Nakamura, K., and Inouye, M. (1981) Preferential selection of deletion mutations of the outer membrane lipoprotein gene of *Escherichia coli* by globomycin. *J. bacteriol*, **145**, 654-656.
20. Giménez, I. M., Dilks, K., and Pohlschröder, M. (2007) *Haloferax volcanii* twin-arginine translocation substates include secreted soluble, C-terminally anchored and lipoproteins. *Mol. Micro.* **66**, 1597–1606
21. van Geest, M., and Lolkema, J. S. (1996) Membrane topology of the sodium ion-dependent citrate carrier of *Klebsiella pneumonia*. Evidence for a new structural class of secondary transporters. *J. Biol. Chem.* **271**, 25582-25589
22. Weiner, J. H., Bilous, P. T., Shaw, G. M., Lubitz, S. P., Frost, L., Thomas, G. H., Cole, J. A., and Turner, R. J. (1998) A novel and ubiquitous system for membrane targeting and secretion of cofactor-containing proteins. *Cell* **93**, 93-101.
23. Kanugula, A. K. K., Repalle, E. R., Pandey, J. P., Sripad, G., Mitra, C. K., Dubey, D. K., and Siddavattam, D. (2011) Immobilization of organophosphate hydrolase on biocompatible gelatine pads and its use in removal of organophosphate compounds and nerve agents. *Indian. J. Biochem. Bio*. **48**, 29-34
24. Ichihara, K., and Fukubayashi, Y. (2010) Preparation of fatty acid methyl esters for gas-liquid chromatography, *J. Lipid. Res*. **51**, 635–640
25. Nadeau O. W., Carlson G. M. (2007) Protein interactions captured by chemical cross-linking: one-step cross-linking with formaldehyde. *CSH Protoc* 2007: pdb prot **4634**
26. Sutherland, B. W., Toews, J., and Kast, J. (2008) Utility of formaldehyde cross-linking and mass spectrometry in the study of protein–protein interactions. *J. Mass. Spectrom*. **43**, 699–715
27. Poole, R. K. (1993) The isolation of membranes from bacteria. Biomembrane Protocols: *Methods in Molecular Biology* **19**, 109-122
28. Schägger, H., and von Jagow, G. (1991) Blue native electrophoresis for isolation of membrane protein complexes in enzymatically active form. *Anal. Biochem*. 199, 223-231
29. Schägger, H. (2006) Tricine–SDS-PAGE. *Nat. Protoc*. **1**, 16-22
30. Kim, M., Kandasamy, K., Chaerkady, R. and Pandey, A. (2010) Assessment of resolution parameters for CID-based shotgun proteomic experiments on the LTQ-Orbitrap mass spectrometer. *J. Am. Soc. Mass. Spectrom.* **21**, 1606–1611
31. Karimova, G., Pidoux, J., Ullmann, A., and Ladant, D. (1998) A bacterial two-hybrid system based on a reconstituted signal transduction pathway. *Proc. Natl. Acad. Sci*. **95,** 5752–5756
32. Zhang, X., and Bremer, H. (1995) Control of the *Escherichia coli* rrnB P1 promoter strength by ppGpp. *J. Biol. Chem*. **270**, 11181-11189
33. Müllerová, D., Krajčíková, D., and Barák, I. (2009) Interactions between *Bacillus subtilis* early spore coat morphogenetic proteins. *FEMS. Microbiol. Lett.* **299**, 74–85.

34. Molloy, M. P., Herbert, B. R., Slade, M. B., Rabilloud, T., Nouwens, A. S., Williams, K. L., Gooley, A. A. (2000) Proteomic analysis of the *Escherichia coli* outer membrane. *Eur. J. Biochem*. **267**, 2871–2881
35. Hatzixanthis, K., Palmer, T., Sargent, F. (2003) A subset of bacterial inner membrane proteins integrated by the twin-arginine translocase. *Mol. Microbiol*. **49**, 1377–1390
36. Keller, R., de Keyzer, J., Driessen, A. J. M., and Palmer, T. (2012) Co-operation between different targeting pathways during integration of a membrane protein. *J. Cell. Biol.* **199**, 303-315
37. Bachmann, J., Bauer, B., Zwicker, K., Ludwig, B., Anderka, O. (2006) The Rieske protein from *Paracoccus denitrificans* is inserted into the cytoplasmic membrane by the twin-arginine translocase. *FEBS J*. **273**, 4817–4830
38. Benning, M. M., Shim, H., Raushel, F. M., Holden, H. M. (2001) High resolution X-ray structures of different metal-substituted forms of phosphotriesterase from *Pseudomonas diminuta*. *Biochemistry* **40**, 2712-2722
39. Thompson, B. J., Widdick, D. A., Hicks, M. G., Chandra, G., Sutcliffe, I. C., Palmer, T., Hutchings, M. I. (2010) Investigating lipoprotein biogenesis and function in the model Gram-positive bacterium *Streptomyces coelicolor*. *Mol. Microbiol.* **77**, 943–957
40. Widdick, D. A., Hicks, M. G., Thompson, B. J., Tschumi, A., Chandra, G., Sutcliffe, I. C., Brulle, J. K., Sander, P., Palmer, T., and Hutchings, M. I. (2011). Dissecting the complete lipoprotein biogenesis pathway in *Streptomyces scabies*. *Mol. Microbiol.* **80**, 1395-1412
41. Beven, L., Le Henaff, M., Fontenelle, C., and Wroblewski, H. (1996) Inhibition of spiralin processing by the lipopeptide antibiotic globomycin. *Curr. Microbiol*. **33**, 317–322
42. Narita, S., and Tokuda, H. (2006) An ABC transporter mediating the membrane detachment of bacterial lipoproteins depending on their sorting signals. *FEBS. Lett.* 580, 1164-1170
43. Sankaran, K., and Wu, H. C. (1993) Lipid modification of bacterial prolipoprotein. Transfer of diacylglyceryl moiety from phosphatidylglycerol. *J. Biol. Chem*. **269**, 19701-19706
44. Rao, N. N., and Torriani, A. (1990) Molecular aspects of phosphate transport in *Escherichia coli*. *Mol. Microbiol*. **4**, 1083-1090
45. Hobbs, E., C, Yin, X., Paul, B. J, Astarita, J. L., Storz, G. (2012) Conserved small protein associates with the multidrug efflux pump AcrB and differentially affects antibiotic resistance. *Proc. Natl. Acad Sci.* **109,** 16696-16701
46. Siddavattam, D., Raju, E. R., Paul, P. V. E., and Merrick, M. (2006) Overexpression of parathion hydrolase in *Escherichia coli* stimulates the synthesis of outer membrane porin OmpF. *Pesticide Biochem. Physiol.* **86,** 146–150.
47. Widdick, D. A., Dilks, K., Chandra, G., Bottrill, A., Naldrett, M., Pohlschroder, M., and Palmer, T. (2006) The twin-arginine translocation pathway is a major route of protein export in *Streptomyces coelicolor*. *Proc. Natl. Acad. Sci*. **103**, 17927-17932
48. Valente, F. M. A., Pereira, P. M., Venceslau, S. S., Regalla, M., Coelho, A. V., Pereira I. A. C. (2007) The [NiFeSe] hydrogenase from *Desulfovibrio vulgaris* Hildenborough is a bacterial lipoprotein lacking a typical lipoprotein signal peptide. *FEBS, Lett.* **581**, 3341-3344
49. Tanaka, S., Narita, S. and Tokuda, H. (2007) Characterization of the *Pseudomonas aeruginosa* Lol System as a Lipoprotein Sorting Mechanism. *J. Biol. Chem*. **282**, 13379-13384
50. Hanahan, D. (1983) Studies on transformation of *Escherichia coli* with plasmids. *J. Mol. Biol.* **166**, 557-580
51. Studier, F. W., Moffatt, B. A. (1986) Use of bacteriophage T7 RNA polymerase to direct selective high-level expression of cloned genes. *J. Mol. Bio.* **189**, 113-130
Simon, R., Priefer, U. and Pühler, A. (1983) A broad host range mobilization system for *in vivo* genetic engineering: transposon mutagenesis in Gram negative bacteria. *Bio/Technology* **1**, 784-790
52. Karimova, G., Dautin, N., Ladant, D. (2005) Interaction network among Escherichia coli membrane proteins involved in cell division as revealed by bacterial two-hybrid analysis. *J. Bacteriol.* **187**, 2233-2243

53. Morales, V. M., Backman, A., and Bagdasarian, M. (1991) A series of wide-host-range low-copy number vectors that allow direct screening for recombinants. *Gene* **97**, 37-47.

FOOTNOTES

[1]To whom correspondence should be addressed: Dayananda Siddavattam, Department of Animal Biology, School of Life Sciences, University of Hyderabad, Prof. C.R Rao Road, Gachibowli, Hyderabad, India 500 046, Tel.: +91 40 23134578; Fax: +91 40 23010120/145; E-mail: sdsl@uohyd.ernet.in

[2]Division of Molecular Microbiology, College of Life Sciences, University of Dundee, Dundee, UK.

[3]The abbreviations used are: OPH, organophosphate hydrolase; OP, Organophosphate insecticides; Tat, Twin arginine transport; SPase, Signal peptidase

FIGURE 1. *OPH remains membrane-associated in the presence of sodium carbonate or urea*- Inner membranes isolated from *B. diminuta* cells were washed with increasing concentrations of either sodium carbonate (Panel A) or urea (Panel B), as indicated. The pellet (P) and supernatant (S) fractions after washing were separated by SDS-PAGE (12.5% acrylamide), and either stained with coomassie blue (upper panels) or blotted and probed with an OPH antibody (lower panels). The untreated membrane (C) is loaded along with the treated samples as a control. M-molecular weight marker.

FIGURE 2. *OPH is a lipoprotein*- (A) Bioinformatic analysis of the OPH signal peptide. The predicted SPaseII cleavage site (green bar), lipo-box (green font) and the invariant cysteine residue (red font) found at the junction of SPaseII cleavage site are shown. Potential SPaseI cleavage sites are indicated with red bars. The twin arginines of the Tat signal peptide are underlined. (B) SDS-PAGE analysis (12.5% acrylamide; upper panel, shown as a loading control) and anti-OPH Western blot (lower panel) of membrane (M) and cytoplasmic (C) proteins extracted from globomycin treated (+) and untreated (-) cells of *B. diminuta* DS010 (pSM5). Lane 5 and 6 show pure mOPH (5) and PreOPH (6) used as molecular size markers. (C) and (D) SDS-PAGE (12.5% acrylamide; upper panel) and corresponding western blot (lower panel) of proteins extracted from periplasmic, cytoplasmic and membrane fractions of *B. diminuta* DS010 containing (C) plasmid pSM5 that produces wild type OPH or (D) plasmid pCSOPH producing OPH^{C24S}. Lanes 4 & 5 indicate mOPH (4) and preOPH (5) used as molecular size markers.

FIGURE 3. *Fatty acids associated with invariant cysteine residue of OPH*- Gas chromatograms of the fatty acid methyl esters extracted from OPH^{C24S} (A) and wild type OPH (B). The novel fatty acid peaks found in the wild type OPH sample are highlighted with boxes. The MS pattern of novel peaks obtained at retention time 17.01(C) and 20.83 (D) and corresponding library search results are shown in (E) for the 17.01 peak and (F) for the 20.83 peak.

FIGURE 4. *Purification of an OPH complex*- (A) and (B) Molecular mass determination of the Ni-affinity purified OPH complex from detergent-extracted membranes by (A) Gel filtration and (B) BN-PAGE. (A) The bold inverted arrows indicate elution volumes of Thyroglobulin (669 kDa), Ferritin (440 kDa), Aldolase (158 kDa), Ovalbumin (44 kDa), Carbonic anhydrase (29 kDa) and Ribonuclease (13 kDa) used to calibrate the column. (B) BN-PAGE analysis (4%-16% acrylamide) of IMAC purified purified OPH complex (Lane 2). Panels C & D BN- PAGE (C) and Tricine-SDS-PAGE (D) analysis of the formaldehyde cross-linked OPH complex purified after delipidation by the extracting the membrane

proteins with methanol:chloroform (3:1). (C) The immunopurified OPH complex is shown in lane 1 and the IMAC purified complex in lane 3. Molecular weight markers are in lane 2. (D) Tricine-SDS-PAGE (4%-16%) profile (left) and corresponding western blots probed using anti-OPH antibodies (right) for immunopurified OPH complex (Lane 2) and IMAC purified complex (Lane 3). Molecular weight markers are in lane 1.

FIGURE 5. *OPH directly interacts with PstS and TolC*- (A) Interactions between the indicated variants of OPH and PstS fused to either the T18 or T25 fragments of *Bordetella pertussis* adenylate cyclase, as indicated. Error bars represent the standard error of the mean (n=3). Also shown are controls performed with either OPH or PstS fused to the T18 fragment tested against the unfused T25 fragment. Significance was assessed using Student's t-test, where * signifies $p < 0.0001$ and ** signifies $p < 0.0001$ relative to the value for T18-PstS + T25 and T18-OPH+ T25, respectively. (B) Tagged variants of OPH and PstS copurify. Lysates of *E. coli* strain ArcticExpress producing $OPH^{CaviTag}$, BirA and $PstS^{C6His}$ (Lane 1), $OPH^{CaviTag}$ and BirA only (Lane 2) or $PstS^{C6His}$ only (Lane 3) were incubated with streptavidin magnetic beads. Following washing to remove non-specifically bound proteins, bound protein was eluted from the beads and analysed by SDS-PAGE (12% acrylamide) and western blotting, probing with anti-OPH (top panel) or anti-His antibodies (bottom panel). Lanes 4 and 5 are control lanes showing total cell lysates prior to treatment of cells producing $PstS^{C6His}$ alone (Lane 4) or $OPH^{CaviTag}$ and BirA only (Lane 5). (C) OPH copurifies with his-tagged TolC. Lysates of *E. coli* strain ArcticExpress producing OPH and $TolC^{N6His}$ (Lane 1), $TolC^{N6His}$ only (Lane 2) or OPH only (Lane 3) were incubated with Ni-charged magnetic beads. Following washing to remove non-specifically bound proteins, bound protein was eluted from the beads and analysed by SDS-PAGE (12.5% acrylamide) and western blotting, probing with anti-OPH (top panel) or anti-His antibodies (bottom panel). Lanes 4 and 5 are control lanes showing total cell lysates prior to treatment of cells producing OPH alone (Lane 4) or $TolC^{N6His}$ alone (Lane 5).

FIGURE 6. *OPH supports growth of B. diminuta using the organophosphate methyl parathion as sole phosphate source*.Panel A and B show growth of *B. diminuta* wild type (■), DS010 (▲), DS010 (pSM5) (●) in minimal medium having either $(NH_4)_2HPO_4$ (panel A) or methyl parathion as sole phosphate source (panel B).

FIGURE 7. *Model for OPH-mediated phosphate acquisition in B. diminuta*- The model includes OPH and its interacting partners TolC, AcrA, PstS and PhoR. The other components of the ABC-type phosphate acquisition system (PstA, PstB and PstC) for which PstS is the periplasmic binding protein are also shown. Entry of the model OP compound to periplasm (1) and its OPH mediated hydrolysis (2) generate alkyl phosphate and *p*-nitrophenol. P_i is generated through the action of periplasmically-located phosphatases/diesterases (3) which binds to PstS (4) and is transported into the cytoplasm by the phosphate specific transport system (5). OM-outer membrane, P-periplasm, IM-inner membrane.

TABLE 1

Strains	**Description**	**Reference**
E. coli DH5α	λ*supE44* Δ*lacU169 (Δ80 lacZΔM15) hsdR17 recA1 endA1 gyrA96 thi1 relA1*	47
E. coli BL21	*hsdS gal(ΔcIts857 ind1 Sam7 nin5) lacUV5 T7 gene1*	48
E. coli S17-1	*thi pro hsd Rhsd MrecA RP4 2-Tc::Mu-Km^r::Tn7 (Tp^r, Sp^r, Sm^r)*	49
BTH101	*F cya-99 araD139 galE15 galK16 rpsL1 (Strr) hsdR2 mcrA1 mcrB1*	50
ArcticExpress	*E. coli B F$^–$ ompT hsdS($r_B^–$ $m_B^–$) dcm$^+$ Tet^r gal endA Hte [cpn10 cpn60 Gent^r]*	Agilent Technologies
B. diminuta	Sm^r, PmB^r , *opd*$^+$	11
B. diminuta DS010	Sm^r, Tc^r, PmB^r, *opd*$^-$ (*opd*::*tet*)	15
Plasmids	**Description**	**Reference**
	Vectors	
pMMB206	Cm^r, broad host range, low copy number, expression vector	51
pGEMT-Easy	Amp^r, TA cloning vector	Promega
pTZ57 R/T	Amp^r, TA cloning vector	Fermentas
pET23b	Amp^r, T7 promoter and a C-terminal 6xHIS-tag	Novagen
pETduet1	Amp^r, contains two multiple cloning sites downstream of T7 promoter.	Novagen
pRSETA	Amp^r, T7 promoter and a N-terminal 6xHIS-tag	
pSM5	Cm^r, complete *opd* gene encoding preOPH, cloned in pMMB206 as *Eco*RI and *Hind*III fragment	13
pKNT25	Plasmid for the expression of C-terminal T25-fusion proteins (Kan^r)	50
pUT18C	pUT18C Plasmid for the expression of N-terminal T18-fusion proteins (Amp^r)	50
pCSOPH	Cm^r, derivative of pSM5 encoding OPH^{C24S}	This work
pOPH141HIS	Cm^r, derivative of pSM5 encoding OPH with 10 histidine residues between 141-142 residues.	This work
pUT18COPH	Amp^r, complete *opd* gene cloned inframe to code for C-terminal T18 fragment.	This work
pUT18CPstS	Amp^r, complete *pstS* gene cloned inframe to code for C-terminal T18 fragment.	This work
pKNT25OPH	Km^r, complete *opd* gene cloned inframe to code for N-terminal T25 fragment.	This work
pKNT25PstS	Km^r, complete *pstS* gene cloned inframe to code for N-terminal T25 fragment.	This work
pOPHV400	Cm^r, Avi tag coding sequence inserted as XhoI and HindIII fragment in pSM5, codes for OPH^{CAviTag}	This work

pAVB400	Amp^r, *opd* variant coding OPH^{CAviTag} taken as EcoRI and HindIII fragment from pOPHV400 and cloned into one of the two multiple cloning sites of pETduet1. The *birA* gene amplified from *E. coli* as NdeI and XhoI fragment was cloned in the second multiple cloning site. Codes for OPH^{CAviTag}, and BirA ligase.	This work
pPST300	Amp^r, the *pstS* amplified from *B. diminuta* as NdeI and XhoI fragment was cloned in pET23b. Codes for PstS^{N6His}	This work
pLPST300	Cm^r, *pstS* amplified from pPST300 as BglII and HindIII fragment cloned in pMMB206 digested with BamHI and HindIII.	This work
pTOLC400	Amp^r, The *tolC* gene amplified from *B. diminuta* cloned as BglII and EcoRI fragment in pRSETA. Codes for TolC^{N6His}	This work
pTLOPH	Cm^r, the *opd* gene amplified as EcoRI and HindIII fragment cloned in pMMB206. Codes for untagged OPH under control of the *tac* promoter.	This work

TABLE 2

Unique Peptides	Peptide sequences	% Coverage	Mr	Accession	Description	Function	Subcellular localization
4	TIVDVSTFDIGR/ASLATGVPVTTHTAASQR/VNPDGMAFIPLR/GVPQE TLAGITVTNPAR/	17	35.7	gi|13786716|	Phosphotriester-ase [B. diminuta]	Unusual substrate specificity for synthetic organophosphate triesters	Plasma membrane
4	SDLPDGILEPQVVR/VILDPAR/IATLGDIDQNAAK/AYNDVNQAVQQIR	4.3	123.3	gi|103485965|	AcrB, acriflavin resistance protein [S. alaskensis RB2256]	Transporter activity	Integral component of membrane
3	LEGVVASLASK/GLAGAFNSNIVK/LTIQYNR	7.2	31	gi|103487768|	F0F1 ATP synthase subunit gamma [S. alaskensis RB2256]	Proton-transporting ATP synthase activity, rotational mechanism	Plasma membrane
2	FTQAGSEVSALLGR/VIDLLAPYAR	2.5	53.9	gi|103487769|	F0F1 ATP synthase subunit beta [S. alaskensis RB2256]	Proton-transporting ATP synthase activity, rotational mechanism	Plasma membrane
2	LELAQYR/LSVGDGIA	1.2	54.4	gi|103487767|	F0F1 ATP synthase subunit alpha [S. alaskensis RB2256]	Proton-transporting ATP synthase activity, rotational mechanism	Plasma membrane
2	LALAEGDLR/VADPSFGVR	1.6	52.6	gi|103487743|	Type I secretion outer membrane protein, TolC [S. alaskensis RB2256]	Outer membrane channel, required for several efflux systems such as AcrAB-TolC, AcrEF-TolC, EmrAB-TolC and MacAB-TolC	Cell outer membrane
2	FDAAGVPNLK/VIGSPGYPAEEER	3	32.2	gi|103487703|	Alpha/beta hydrolase [S. alaskensis RB2256]	Hydrolase activity/ aromatic compounds	Unknown
2	LPAVAISVFG/ISAVGSSTV	3	34.2	gi|159795674|	Phosphate Preplasmic Binding Protein Psts [Y. Pestis]	Phosphate binding periplamsic component	Periplasm

FIGURE 1

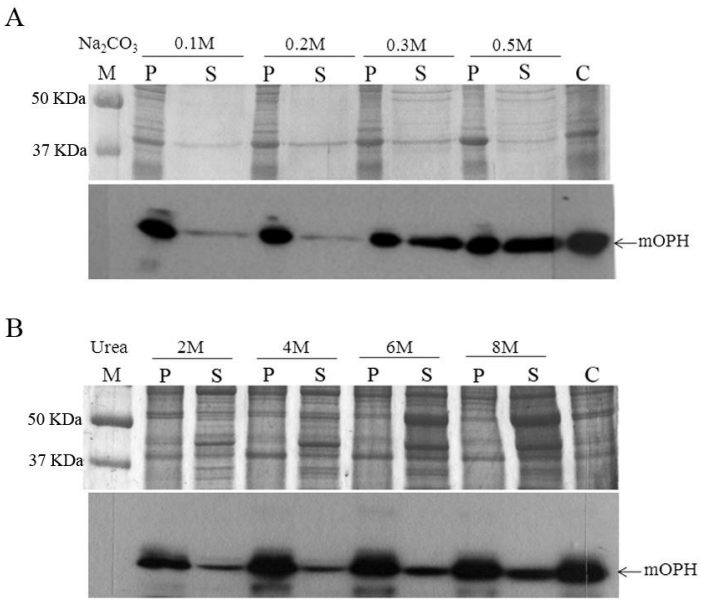
A
Na_2CO_3
0.1M
0.2M
0.3M
0.5M
M
P
S
P
S
P
S
P
S
C
50 KDa
37 KDa
mOPH
B
Urea
2M
4M
6M
8M
M
P
S
P
S
P
S
P
S
C
50 KDa
37 KDa
mOPH

FIGURE 2

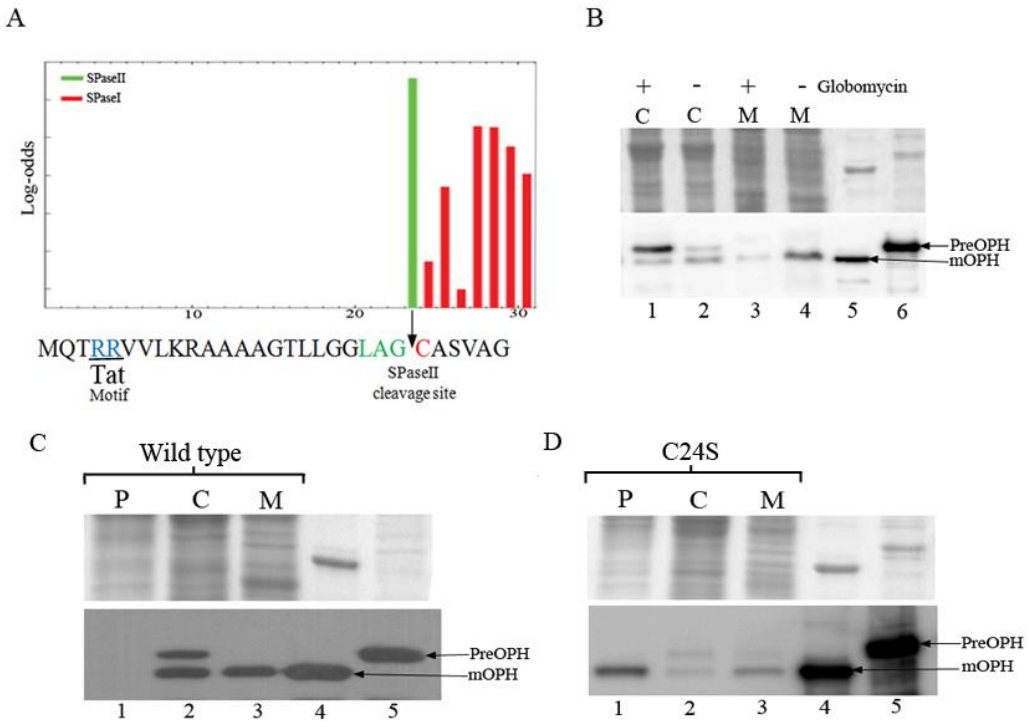
A
SPaseII
SPaseI
Log-odds
10
20
30
MQTRRVVLKRAAAAGTLLGGLAGCASVAG
Tat
Motif
SPaseII
cleavage site
B
+ - + - Globomycin
C C M M
PreOPH
mOPH
1 2 3 4 5 6
C
Wild type
P C M
PreOPH
mOPH
1 2 3 4 5
D
C24S
P C M
PreOPH
mOPH
1 2 3 4 5

FIGURE 3

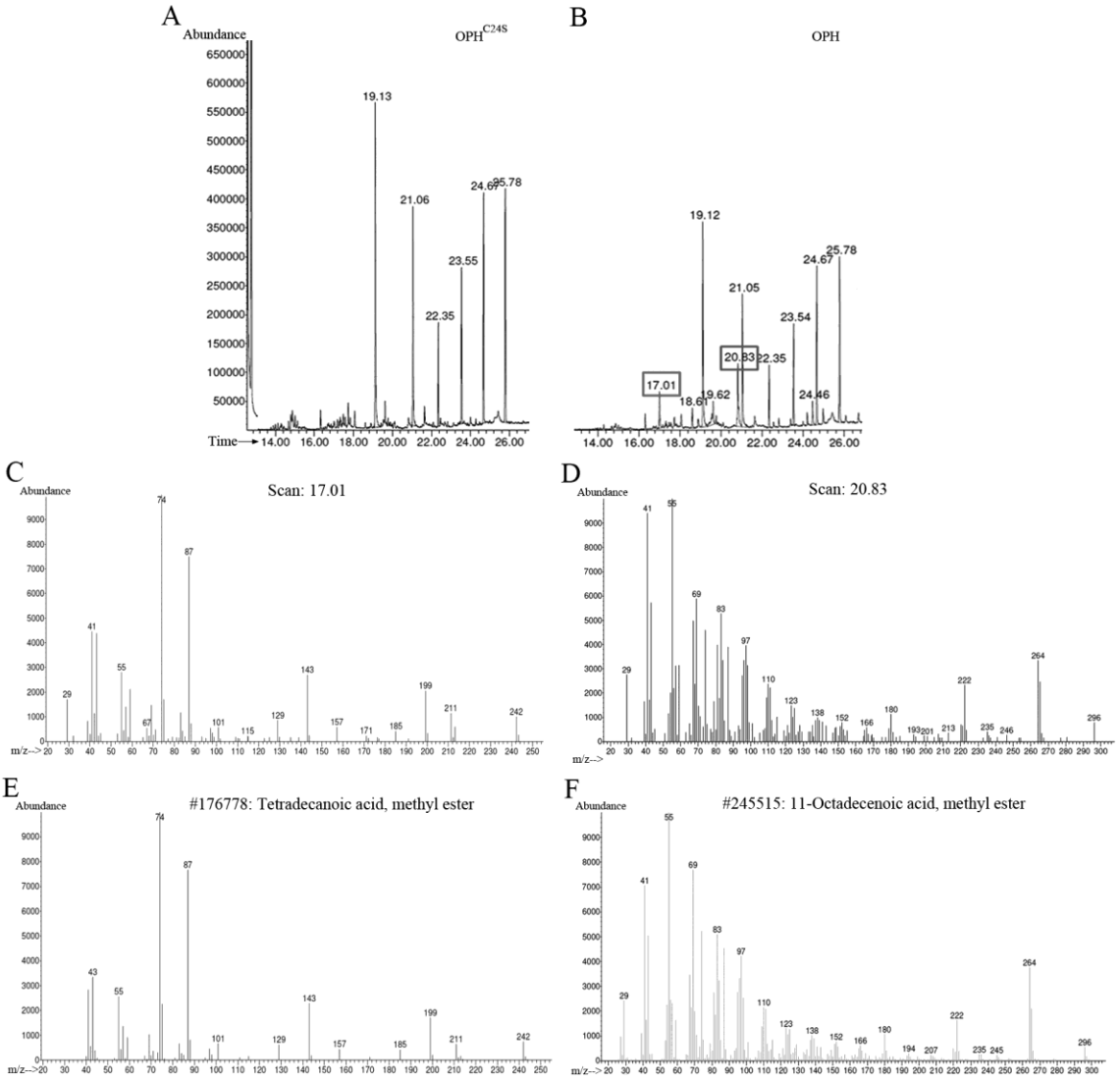
A
Abundance
OPH^C24S
19.13
21.06
23.55
22.35
24.67
25.78
Time
B
OPH
19.12
25.78
24.67
21.05
23.54
20.83
22.35
17.01
19.62
18.61
24.46
C
Abundance
Scan: 17.01
D
Abundance
Scan: 20.83
E
Abundance
#176778: Tetradecanoic acid, methyl ester
F
Abundance
#245515: 11-Octadecenoic acid, methyl ester
m/z-->

FIGURE 4

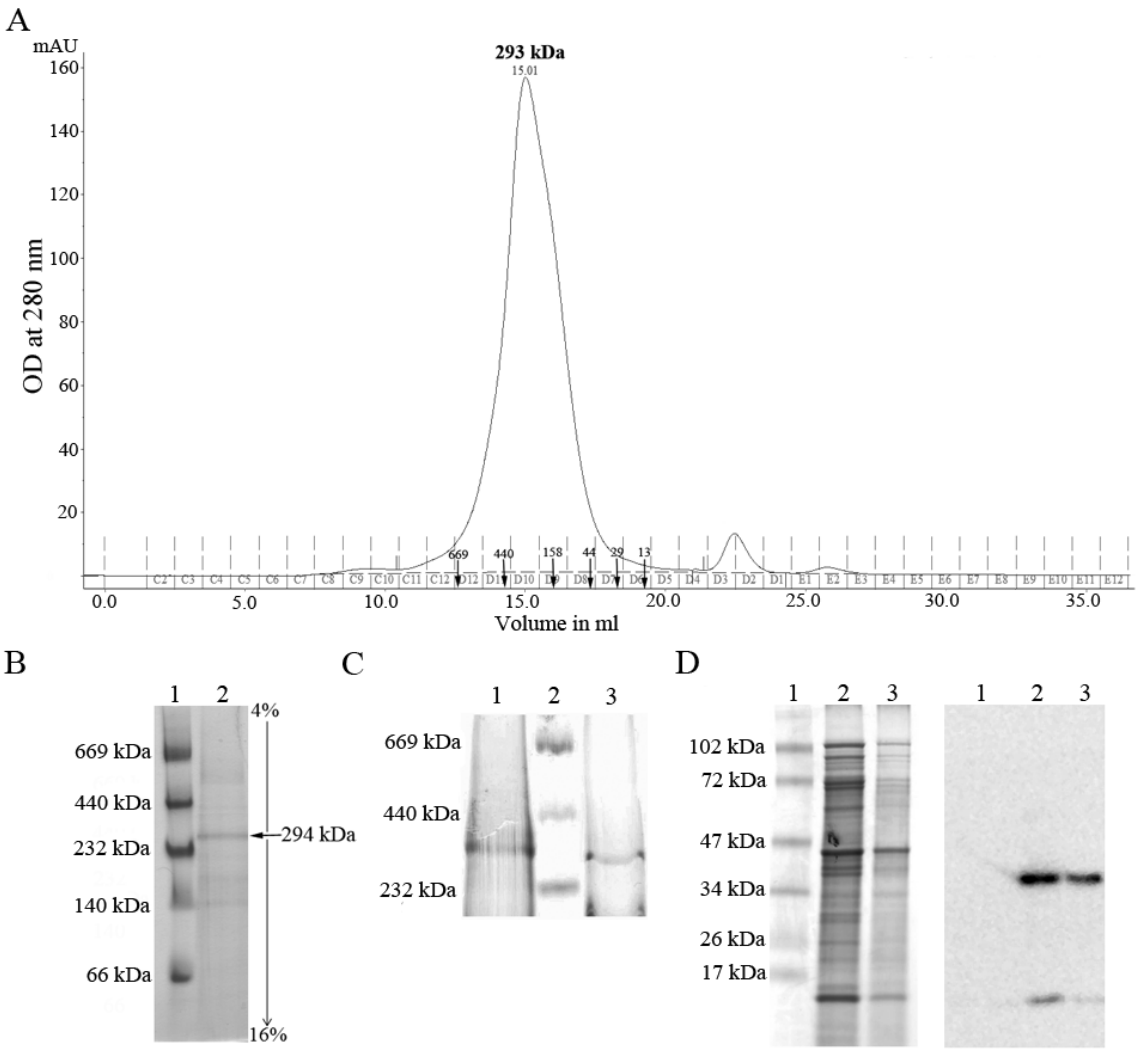
A
mAU
293 kDa
15.01
OD at 280 nm
669
440
158
44
29
13
Volume in ml
B
1 2
4%
669 kDa
440 kDa
232 kDa
140 kDa
66 kDa
294 kDa
16%
C
1 2 3
669 kDa
440 kDa
232 kDa
D
1 2 3
102 kDa
72 kDa
47 kDa
34 kDa
26 kDa
17 kDa
1 2 3

FIGURE 5

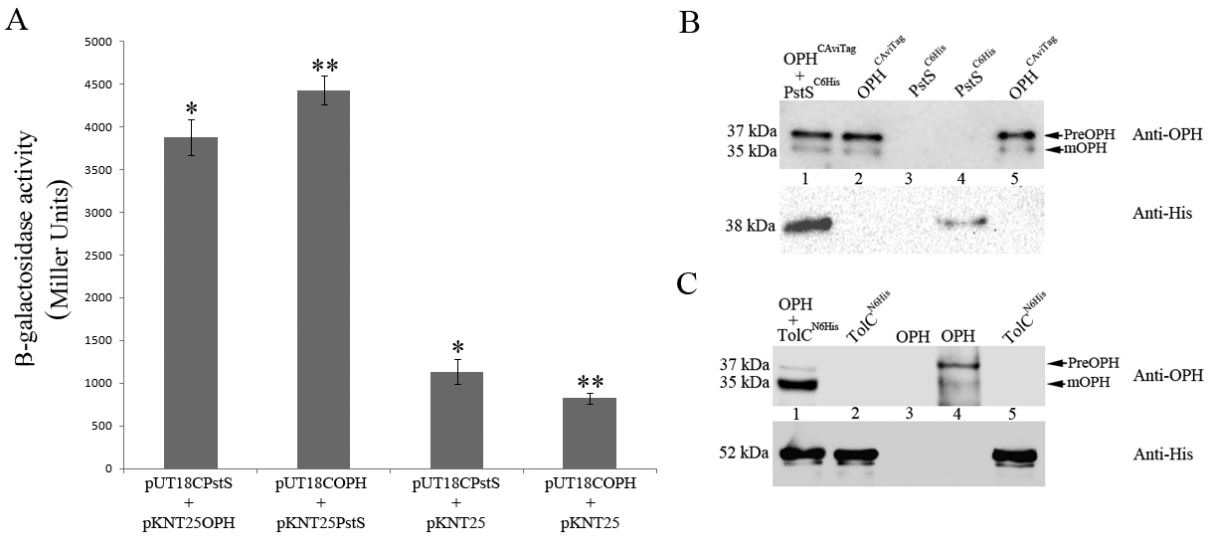
A
β-galactosidase activity (Miller Units)
5000
4500
4000
3500
3000
2500
2000
1500
1000
500
0
*
**
*
**
pUT18CPstS + pKNT25OPH
pUT18COPH + pKNT25PstS
pUT18CPstS + pKNT25
pUT18COPH + pKNT25
B
OPH CAviTag + PstS C6His
OPH CAviTag
PstS C6His
PstS C6His
OPH CAviTag
37 kDa
35 kDa
PreOPH
mOPH
Anti-OPH
1 2 3 4 5
38 kDa
Anti-His
C
OPH + TolC N6His
TolC N6His
OPH
OPH
TolC N6His
37 kDa
35 kDa
PreOPH
mOPH
Anti-OPH
1 2 3 4 5
52 kDa
Anti-His

FIGURE 6

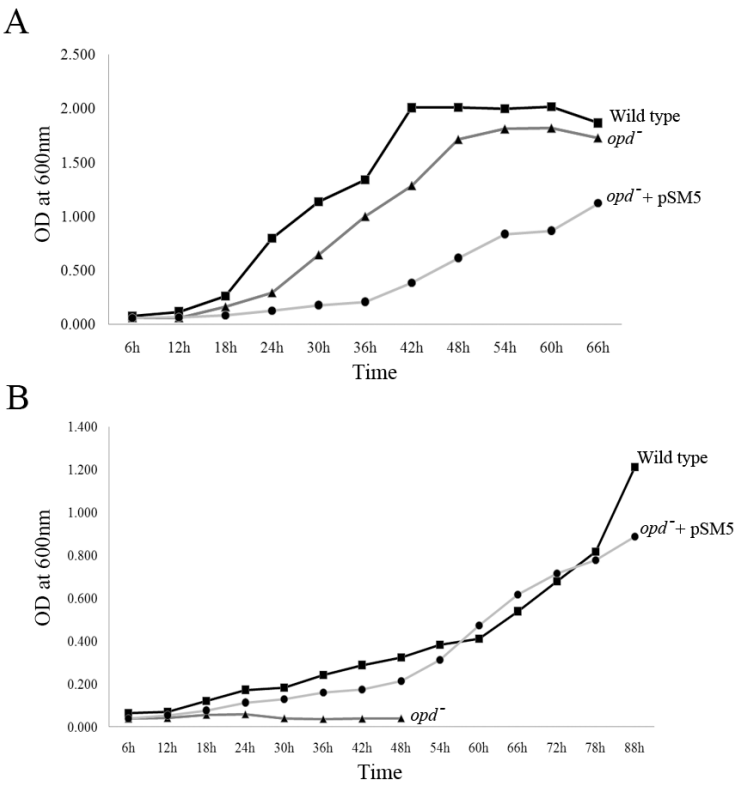
A
2.500
2.000
1.500
1.000
0.500
0.000
OD at 600nm
6h
12h
18h
24h
30h
36h
42h
48h
54h
60h
66h
Time
Wild type
opd⁻
opd⁻ + pSM5
B
1.400
1.200
1.000
0.800
0.600
0.400
0.200
0.000
OD at 600nm
6h
12h
18h
24h
30h
36h
42h
48h
54h
60h
66h
72h
78h
88h
Time
Wild type
opd⁻ + pSM5
opd⁻

FIGURE 7

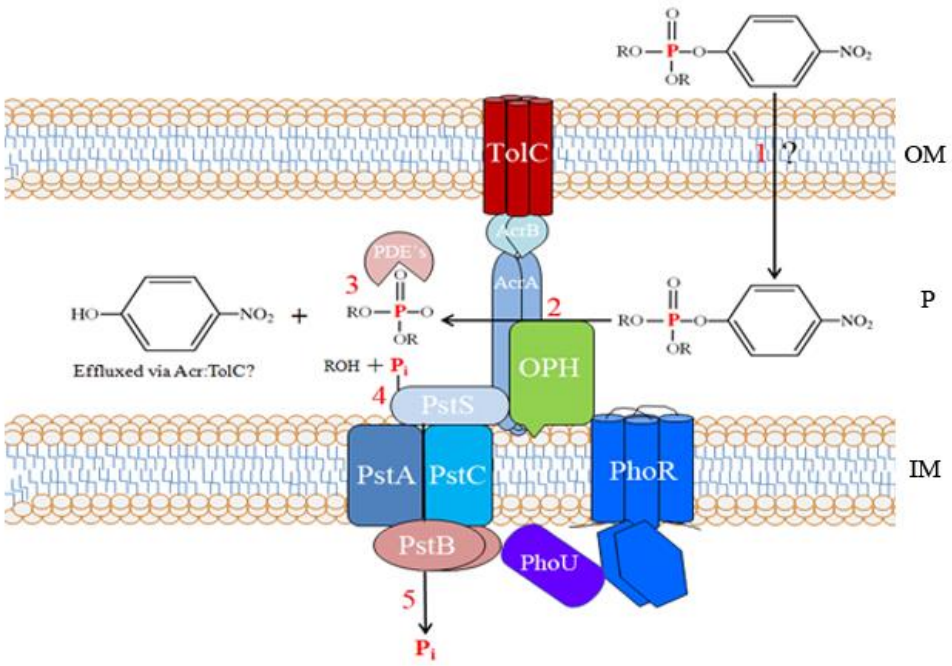
TolC
AcrB
AcrA
PDE A
OPH
PstS
PstA
PstC
PstB
PhoR
PhoU
OM
IM
P
1 ?
2
3
4
5
Effluxed via Acr:TolC?
ROH + Pi
Pi